Materials and Design 54 (2014) 660–669

Contents lists available at ScienceDirect

Materials and Design

journal homepage: www.elsevier.com/locate/matdes

Effect of fibre coating and geometry on the tensile properties of hybrid carbon nanotube coated carbon fibre reinforced composite

M.A. Shazed [a], A.R. Suraya [a,b,*], S. Rahmanian [b], M.A. Mohd Salleh [a,b]

[a] Department of Chemical and Environmental Engineering, Faculty of Engineering, University Putra Malaysia, Selangor 43400, Malaysia
[b] Nanotechnology and Nanomaterials Group, Materials Processing and Technology Laboratory, Institute of Advanced Technology, University Putra Malaysia, Selangor 43400, Malaysia

ARTICLE INFO

Article history:
Received 30 May 2013
Accepted 18 August 2013
Available online 27 August 2013

Keywords:
Hybrid composite
Carbon nanotubes
Mechanical property
Chemical vapor deposition
Fibre orientation distribution

ABSTRACT

Hierarchically structured hybrid composites are ideal engineered materials to carry loads and stresses due to their high in-plane specific mechanical properties. Growing carbon nanotubes (CNTs) on the surface of high performance carbon fibres (CFs) provides a means to tailor the mechanical properties of the fibre–resin interface of a composite. The growth of CNT on CF was conducted via floating catalyst chemical vapor deposition (CVD). The mechanical properties of the resultant fibres, carbon nanotube (CNT) density and alignment morphology were shown to depend on the CNT growth temperature, growth time, carrier gas flow rate, catalyst amount, and atmospheric conditions within the CVD chamber. Carbon nanotube coated carbon fibre reinforced polypropylene (CNT-CF/PP) composites were fabricated and characterized. A combination of Halpin–Tsai equations, Voigt–Reuss model, rule of mixture and Krenchel approach were used in hierarchy to predict the mechanical properties of randomly oriented short fibre reinforced composite. A fractographic analysis was carried out in which the fibre orientation distribution has been analyzed on the composite fracture surfaces with Scanning Electron Microscope (SEM) and image processing software. Finally, the discrepancies between the predicted and experimental values are explained.

1. Introduction

The area of hybrid fibre-reinforced polymeric composites has received considerable interest by the engineering community because of its unique structure and mechanical properties [1,2]. Carbon fibre (CF) reinforced polymeric composites have a wide range of unexplored potential applications in various technological areas such as aerospace, automobile, electronic and process industries due to their outstanding properties, such as high specific strength and stiffness, lower weight and flexible tailoring [3]. Recently, CF reinforced polymer composites incorporating carbon nanotubes (CNTs) have attracted significant interest due to their extensive applications that conventional CF reinforced composites cannot offer [4,5]. In this paper the major focus was on developing 'CNT-coated short carbon fibre reinforced polypropylene (CNT-CF/PP)' hybrid composites due to their advantages at being strong, lightweight engineering materials at a relatively low cost. Polypropylene (PP) was the preferred reinforcing polymer since it is a member of the group of commodity thermoplastics synthesized in large quantities and not very responsive to chemical stress cracking. Recent potential applications for CF reinforced PP composites involves body structures and interior trim for passenger cars, fuel cells, fuel tanks and several other structural uses [6,7]. Short fibre reinforced composites are attractive due to their simplicity of fabrication and relatively low cost synthesizing methods [8]. The composites consist of randomly orientated short fibres in a continuous polymeric matrix, the orientation of the fibres depending on the processing techniques and conditions employed [9].

The tensile and interfacial properties of hybrid (CNT-CF/PP) composites are largely affected by the CNT which are directly grown onto the fibre surface. It is desirable to develop a one-step coating process whereby CNT grow directly onto the CF without the need for CF pre-treatment or CNT purification after treatment. This one-step process has been attempted by using a floating catalyst CVD [10,11]. To prepare the short fibre reinforced composite, mixed blending is one of the extensively used fabrication method available. The composite can be developed in the form of sheets by using hot or cold compression molding [12,13]. A number of static mechanical test procedures can be employed in order to evaluate the mechanical properties of composites. For example, tensile tests measure the modulus and strength of composites under a static or slowly applied force, flexural tests evaluate the strength of composites under the application of bending load and Izod impact tests determine the impact strength when a kinetic

* Corresponding author at: Nanotechnology and Nanomaterials Group, Materials Processing and Technology Laboratory, Institute of Advanced Technology, University Putra Malaysia, Selangor 43400, Malaysia. Tel.: +60 3 89466285; fax: +60 3 86567120.
E-mail address: suraya_ar@upm.edu.my (A.R. Suraya).

0261-3069/$ - see front matter © 2013 Elsevier Ltd. All rights reserved.
http://dx.doi.org/10.1016/j.matdes.2013.08.063

energy is employed to create fracture on the composite [14]. Tensile testing is the most frequently employed material evolution test method as this provides basic design information on the strength of the materials [15]. As the strength and stiffness of a material increases, the dimensions and consequently the mass of the material needed to carry a certain load bearing application is reduced [16].

However, it is important to theoretically predict the tensile properties of composite in order to validate and improve the reliability of experimental results. Theoretical prediction of the mechanical properties of a fibre-reinforced composite has been an active research area for the past couple of decades. Several models have been proposed for the prediction of composite mechanical properties from those of the constituent fibre and matrix. The predictions for the elastic properties, however, show significant scatter depending upon the assumed geometrical orientation of fibres inside the composite. Experimental determination of the randomly oriented fibre reinforced composite moduli is difficult, especially when it involves determining the longitudinal and transverse modulus. Thus, theoretical models like Halpin and Panago [17] can be utilized to mathematically model the composite as a laminated system. The mathematical model named Halpin–Tsai model is most likely to predict the elasticity of composite material based on the geometry and orientation of the filler and the elastic properties of the filler and matrix. This model is based on the self-consistent field method but often considered being empirical. Through Halpin–Tsai equations, the modulus of the composite can be studied with the correlation of geometric and mechanical characteristics of the CNT-CF and mechanical properties of PP matrix [18]. A couple of equations were stated by Halpin and Tsai for randomly oriented short fibre reinforced composites [19]:

$$E_{11} = E_M\left(\frac{1 + c\eta_{11}v_f}{1 - \eta_{11}v_f}\right), \quad \text{where} \quad \eta_{11} = \frac{(E_f/E_M) - 1}{(E_f/E_M) + c} \tag{1}$$

$$E_{\perp} = E_M\left(\frac{1 + \alpha\eta_{\perp}v_f}{1 - \eta_{\perp}v_f}\right), \quad \text{where} \quad \eta_{\perp} = \frac{(E_f/E_M) - 1}{(E_f/E_M) + \alpha} \tag{2}$$

Here, E_{11} and $E_{\perp}$ is the longitudinal and transverse modulus, η_{11} and $\eta_{\perp}$ describes the longitudinal and transverse efficiency factors, c is the shape factor governing the fibre aspect ratio, (l/d), E_M is Young's modulus of the matrix, E_f is Young's modulus of the fibre, v_f is the volume fraction and α is denoting a geometric factor.

The properties of randomly oriented short fibre reinforced composites depend upon the shape of the heterogeneities, upon the volume fraction occupied by them, and upon the interface among the constituents [20]. If the fibres are not continuous, an allowance must be made for the fact that each short fibre is unable to carry stress near its ends, load being transmitted into the fibres by shear along the fibre/matrix interface. However, the influence of this length is ineffective if the fibres are longer than about 50 times the diameter [21]. Combined Voigt–Reuss model describes the elastic properties of composites with randomly oriented fibre distribution, based upon those particular characteristics [22]. In this model, the overall Young's modulus E_c of the composite with two constituents in the specified load direction is given by:

$$E_C = \frac{3}{8}E_{11} + \frac{5}{8}E_{\perp} \tag{3}$$

E_c is the Young's modulus of composite.

Complex internal geometrical structures are generally developed with the short fiber reinforced composites after fabricating. The complexity of the rheological behavior of such composite materials accomplished with the complex geometries usually requires the use of either experiments or theoretical analysis to predict the final morphology of a selected differential part and to relate whole composite structure to the properties of that specific part [23]. The most common approach consists of modifying the classical rule-of-mixtures (RoMs) to describe the tensile properties of randomly oriented fibre reinforced composites:

$$E_c = E_M(1 - v_f) + \eta_L\eta_0E_f v_f \tag{4}$$

which is incorporated with the Krenchel equation:

$$\eta_0 = \sum_n a_{fn}\cos^4\alpha_n / \sum_n a_{fn}, \quad \text{where} \sum_n a_{fn} = 1 \tag{5}$$

Here, η_L is the fibre-length correction factor ($\sim$1), η_0 is described as the Krenchel orientation efficiency factor [20], a_{fn} is the ratio between the cross-sectional area presented by a group of fibres oriented at an angle to the applied load direction and the total area of all the fibres at a given cross section of the composite, and $n = 1, 2, 3, 4, \ldots, n$.

Throughout the paper, we report the elastic properties of CNT-CF/PP composites evaluated by both theoretical and experimental methods. The aims of the present research work were, (1) to execute the CNT-CF/PP composite tensile properties (Young's modulus, tensile strength and stiffness) through a theoretical explanation; (2) to validate the experimental results with respect to the theoretical findings in search of a better correlation.

2. Experimental procedure

2.1. Carbon fibre surface coating by CNT

The growth of CNT on commercially-available, unsized, polyacrylonitrile (PAN)-based carbon fibres (Toho Tenax America, Inc.) was carried out in a horizontal tubular quartz furnace using a custom built CVD unit. Fig. 1 shows the schematic diagram of the CVD process with the inlet and outlet components.

Neat carbon fibre tows were placed inside the quartz reactor in the isothermal heating zone. The reactor was then purged with argon. Subsequently, the furnace was switched on to heat the furnace to the desired temperature at the rate of 12 °C/min. The schematic diagram of the temperature profile and supporting gas flow rates for CNT growth on CF is illustrated in Fig. 2.

A uniform solution of benzene (system, 99% purity) and ferrocene (acros, 98% purity) was prepared in a conical flask using a mixing ratio of 2 g ferrocene/50 ml benzene. Benzene and ferrocene was used as the carbon source and catalyst precursor respectively. Then, hydrogen was used as the carrier gas to entrain the benzene/ferrocene vapor into the reactor. The flow rate for both argon and hydrogen gases was fixed at 100 ml/min while the reaction time for the CNT-coating process was carried out for 30 min. The coating process was carried out at 700 °C as well as800 °C in an inert argon atmosphere. At the end of the reaction, the hydrogen supply was stopped and the argon flow was restarted during the cooling process of the furnace to room temperature. Finally, the CNT coated CF samples were taken out for conducting characterizations and fabrication of composite. The structural and morphological features of the CNT coating were analyzed using Scanning Electron Microscope (SEM).

2.2. Composite fabrication, tensile testing and analysis

Composite specimens were fabricated using chopped CF with an average length of 2 mm before and after coating with CNT compounded with PP (Titan PP polymers (M) Sdn. Bhd.) matrix. A 10 wt% of CNT-CF was used throughout the overall amount of 40 g compounding. A screening process was done at an earlier stage of melt blending process in order to determine the optimum equipment parameters for producing homogeneous composite, such as blending temperature, time and roller rotor speed. After a few trial observations, the compounding process was carried out in an internal mixer (Thermo Haake Polydrive R600/610) at a

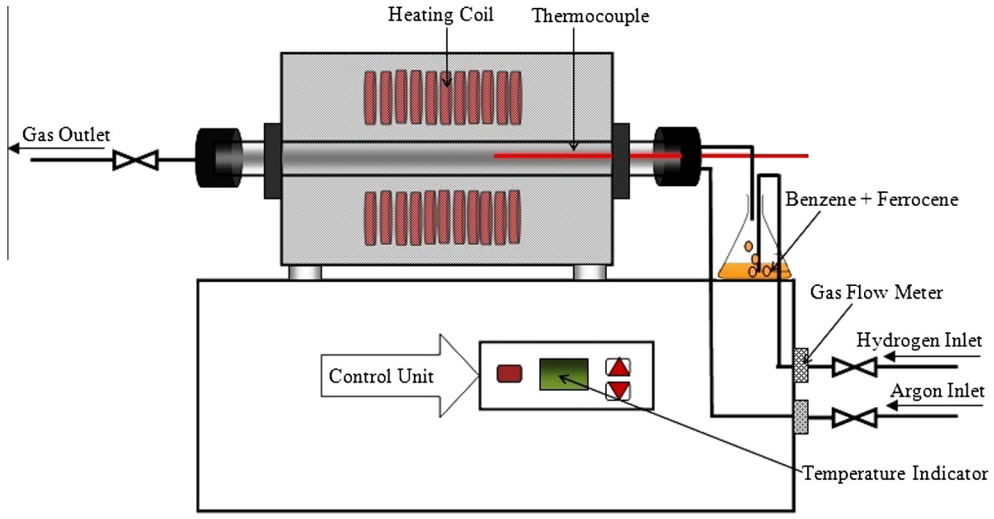

Fig. 1. Schematic diagram of a custom built floating catalyst CVD.

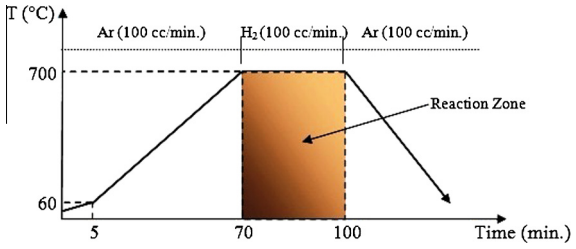

Fig. 2. Temperature profile and gas flow in CVD.

temperature of 170 °C with a rotor speed of 50 rpm. The compounded material and the interface between the matrix and fibres was roughly observed using Polarized Light Microscope. This attempt helps to check the uniformity of fibres inside the matrix and the surface adhesion between the matrix and short fibres. After applying hot press compression moulding the composite was then ready for testing and characterization. The sheets of composites produced by using compression moulding were cut into a dumbbell shape with a recommended size by ASTM: D-638 in order to undergo tensile testing. Tensile tests (Instron Universal Testing Machine 4302) were carried out using a load capacity of 1 kN at a crosshead speed of 5 mm/min as described in ASTM: D-638 [24]. The fracture surface of composite was analyzed by SEM to examine the fibre orientation distribution inside the composite. The schematic diagram of the methodology used for the synthesis and tensile testing of CNT-CF/PP composite starting from CNT growth on CF is illustrated in Fig. 3. Single fibre fragmentation tests [25] were also carried out to determine interfacial shear strength (IFSS) between the hybrid fibres and epoxy polymer matrix.

2.3. Fracture surface geometry

The geometry of the models and the governing equations adopted in the present study are the same as those employed in the rule-of-mixtures (RoMs) and Krenchel approach. For short fibre reinforced composites with small aspect ratio and low volume fraction, the fibres can be modeled as straight cylinders. A small differential area of fabricated composite with three model fibres is illustrated in Fig. 4(a). Fig. 4(b) shows a short fibre in 3D space as a cylinder which is described by the centre point, C, orientation angle, α, diameter, d and length, l. For 3D randomly oriented short fibres, the geometric factor, α is 1/6 [21].

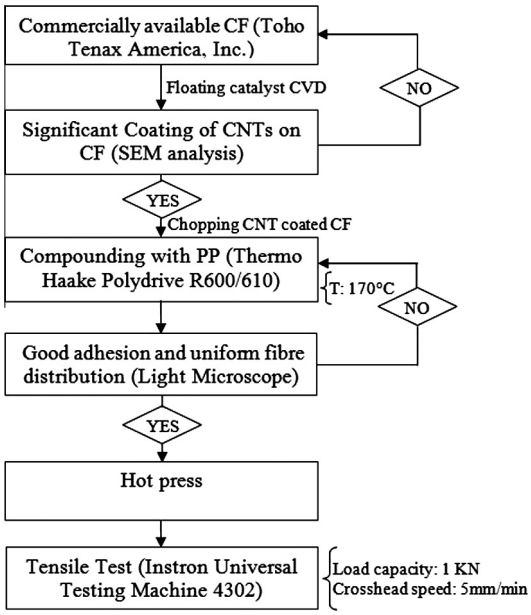

Fig. 3. Hierarchical flow chart of the methodology used to fabricate CNT-CF/PP composite.

The fractographic study of the composite's fracture surface was conducted using SEM. A thorough analysis was done on the fibres of fracture surface using Bersoft and Geozebra image analyzing software packages to evaluate the geometric features such as fibre orientation distribution factor η_0.

2.4. Implementation of mathematical models

In order to perform model based evaluation, some assumptions can be developed: (1) the matrix is isotropic in behaviour (matrix orientation that may affect the tensile properties and any other load transferred from the matrix to the fibre is excluded), (2) longitudinal modulus is dependent on the shape factor, (3) transverse modulus is dependent on the geometric factor for randomly oriented short fibres, (4) there is a negligible difference between fibre volume fraction in CNT-CF/PP composite and CF/PP composite.

To predict the composite properties, Halpin–Tsai equations, combined Voigt–Reuss model, simple rule-of-mixtures (RoMs) and Krenchel approach were used in hierarchy, as shown in Fig. 5.

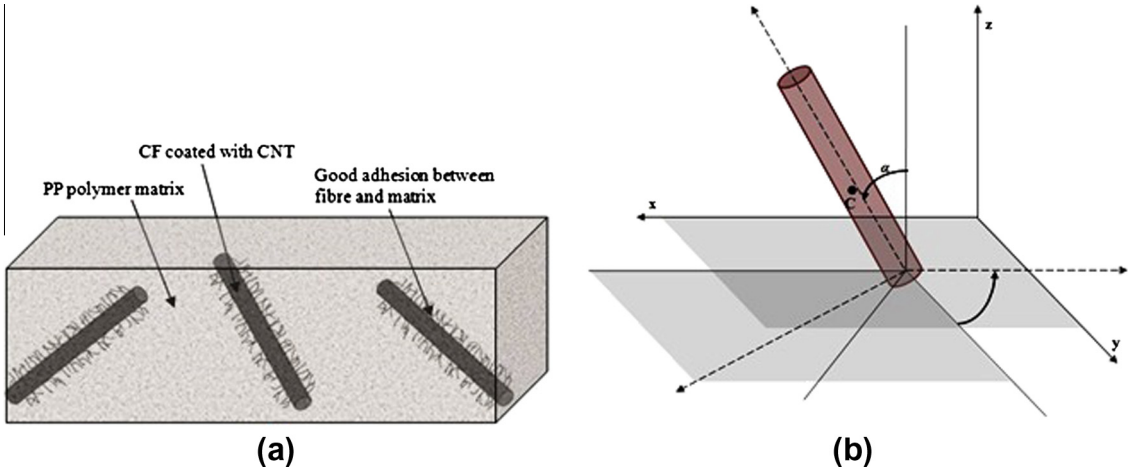

Fig. 4. Schematic illustrations (a) CNT-CF/PP composite with three model fibres (not to scale) and (b) a cylindrical model fibre in 3D space.

Initially, Halpin–Tsai equations were implemented to estimate the tensile properties of CNT reinforced PP composite. These composite properties were then utilized to evaluate the mechanical properties of CNT-CF/PP composite taking into consideration fibre geometry. In this approach, mechanical properties of CNT reinforced PP composite were used as the properties of the matrix [26]. The coating of CNT on CF not only increases the IFSS, but also contributes to strengthen the neighborhood matrix according to CNT length and dispersion [27]. Modified Halpin–Tsai equations to evaluate the tensile properties of CNT reinforced PP composites are given as [28]:

$$E_C = \frac{3}{8}\frac{1+2\left(\frac{l_{CNT}}{d_{CNT}}\right)\left(\frac{\left(\frac{E_{eq}}{E_M}\right)-1}{\left(\frac{E_{eq}}{E_M}\right)+2\left(\frac{l_{CNT}}{d_{CNT}}\right)}\right)V_f}{1-\left(\frac{\left(\frac{E_{eq}}{E_M}\right)-1}{\left(\frac{E_{eq}}{E_M}\right)+2\left(\frac{l_{CNT}}{d_{CNT}}\right)}\right)V_f}\times E_M+\frac{5}{8}\times\frac{1+2\left(\frac{\left(\frac{E_{eq}}{E_M}\right)-1}{\left(\frac{E_{eq}}{E_M}\right)+2}\right)V_f}{1-\left(\frac{\left(\frac{E_{eq}}{E_M}\right)-1}{\left(\frac{E_{eq}}{E_M}\right)+2}\right)V_f}\times E_M \quad (6)$$

Volume fraction of the coated fibres reinforced composite is given by the equation:

$$w_f = \frac{w_f/\rho_f}{(w_f/\rho_f)+(w_M/\rho_M)} \quad (7)$$

Here, w_f and w_M are the weight fraction of filler and matrix respectively. Table 1 shows the parameters and numerical values that are utilized in the process.

When the composite's internal geometry was a major concern RoM was utilized to analyze the fibre orientation distribution factor η_0. To yield the through-thickness fibre orientation efficiency, the Krenchel equation was modified to:

$$\eta_0 = \frac{N_{f1}\cos^3\alpha_1 + N_{f2}\cos^3\alpha_2 + N_{f3}\cos^3\alpha_3 + \ldots + N_{fn}\cos^3\alpha_n}{N_{f1}\sec\alpha_1 + N_{f2}\sec\alpha_2 + N_{f3}\sec\alpha_3 + \ldots + N_{fn}\sec\alpha_n} \quad (8)$$

Here, the notation N_{f1} represents the fraction of the total number of fibres (N_f) orientated at angle α_1 in any field of view. Thus measuring the through-thickness fibre orientation angles, using a series of fields-of-view and calculating corresponding efficiency factors will allow the overall modulus of composite to be determined.

The schematic diagram of constructive numerical evaluation process for Young's modulus is illustrated in Fig. 6.

Young's modulus of CF and PP was determined to be 231 GPa and 1.5 GPa respectively. Short fibre length, l, was 2 mm and diameter, d, was 6 μm. CF weight fraction was 10%, and the remaining PP matrix weight fraction was 90%. The resulting data was used for comparison with the experimental results obtained from tensile testing.

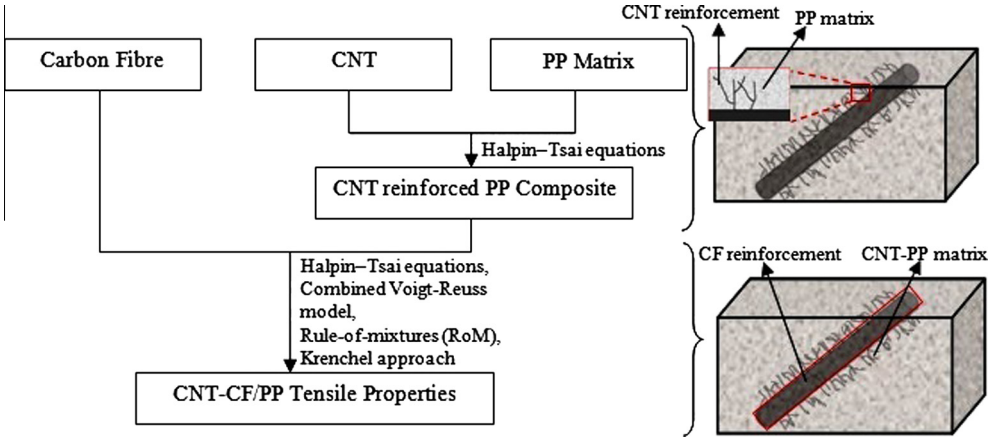

Fig. 5. Schematic diagram of hierarchical approach to evaluate the mechanical properties of hybrid CNT-CF/PP composite.

Table 1
The parameters used for model based prediction.

Parameters	Carbon fibre (CF)	CNT	PP
Young's modulus (E)	231 GPa	1 TPa	1.5 GPa
Diameter (d)	6 μm	30 nm	–
Average length in composite (l)	2 mm	20 μm	–
Shape factor (c)	666.67	–	–
Density	1.8 gm/cm^3	2.25 gm/cm3	0.9 gm/cm^3
Weight fraction in composite (w_f)	0.09	1.71×10^{-3}	–
Volume fraction in composite (υ_f)	0.052	6.83×10^{-4}	–
Wall thickness (t)	–	1.5 nm	–
Equivalent modulus (E_{eq})	–	200 GPa	–

3. Results and discussions

3.1. Characteristic features of the CNT coated CF

Fig. 7 shows representative SEM images of as received CF and CNT coated CF. It can be seen from Fig. 7(b) and (c) that CNT were able to grow intensively on the surface of CF at temperatures of 800 °C and 700 °C. The high density of CNT is desirable due to the purpose of producing high performance fibre reinforced composites [29]. However the coatings were found to be more uniform with minimal clumping and agglomeration at the latter temperature. It was deduced that under the current experimental conditions, the higher temperature led to a higher degree of catalyst agglomeration which affected the homogeneous growth of CNT. Furthermore, a lower synthesis temperature is desirable to minimise heating energy and to protect the CF from being damaged by unnecessary high heat level. The inset in Fig. 7(c) shows a TEM image of CNT on the coating surface, which indicates that the CNT are of the multi walled type. After 30 min of reaction time, it can be seen from Fig. 7(d) that a coating with an apparent thickness of 3 μm has been achieved.

These SEM and TEM images show that the CNT grow in a random manner creating a thick and multi-branched CNT network. The formation of multi-branched CNT is believed to be dependent on the effects of temperature, carrier gas flow rate and catalyst concentration [30]. The random tree-like CNT branches largely dominate to increase the structural properties of their reinforcing hybrid composites. Other researchers have shown that CNT were grown perpendicular to the fibre surface using catalyst impregnation approach [31]. The randomness of produced CNT is probably due to the floating catalyst technique [11]. For the purpose of making randomly orientated short fibre reinforced nanocomposites, the direction of CNT growth is not of a major concern. This is because the CNT coating provides a means of improving IFSS of the hybrid fibre as well as additional reinforcement to the overall composite. Single fibre fragmentation tests show that the IFSS between the hybrid fibre and epoxy matrix is 18.10 MPa, compared to 12.52 MPa for neat CF. This value is comparable to the IFSS obtained by Hui and co-workers in which the CNT were known to be strongly grafted onto the fibre surfaces [25]. The IFSS of the hybrid fibre demonstrates that the CNT are firmly anchored to the fibre surface.

3.2. Tensile properties of CNT-CF/PP composite

In the context of this work, the CF treatment condition using a reaction temperature of 700 °Cand 30 min reaction time was able to produce a composite with relatively higher tensile modulus and strength compared to the neat CF/PP composite. Thus the tensile properties of composite incorporated by the coated fibres with this specific reaction condition were considered to be analyzed. Fig. 8 shows the tensile behavior of neat CF/PP and CNT-CF/PP composites when applied under tensile loading. It can be seen from Fig. 8(a) that the tensile modulus of neat-CF/PP and CNT-CF/PP were found to be 1.72 and 3.52 GPa respectively. In Fig. 8(b), the maximum height refers to the tensile strength of composite. The highest peak of the curve indicates the maximum load that the composites specimen could withstand without fracturing which also refers to the tensile strength of composite. The steeper slope indicates the increasing stiffness of the composite. According to the experimental observation, neat-CF/PP and CNT-CF/PP composites showed a tensile strength of 20.5 and 33.63 MPa respectively. In contrast with the neat-CF/PP a composite, the tensile modulus of CNT-CF/PP composites has enhanced by approximately 104% and tensile strength increased to approximately 64%. The results can be compared with that found by Sharma and Lakkad where composites fabricated from CNT-coated CF showed 69% higher tensile strength as compared to composites made of neat-CF [32]. The enhanced tensile properties are likely to be the overall effect of CF surface coating by CNT. CNT have dominated as the interfacial binder in between the carbon fibre and PP matrix; as well as being the additional supporting reinforcement for the hybrid composites [26].

3.3. Fibre orientation distribution in 3D space

Fig. 9 shows the fibre orientation distribution on the fractured surface of different composite samples. The procedure is demonstrated by Laspalas and co-workers where local fibre orientation distribution has been measured by means of SEM analysis of the composite interior and image processing software [33]. From the distribution pattern it can be demonstrated that the CF are oriented in a random manner inside the composite. The fibre orientation efficiency factor is considered with the transverse

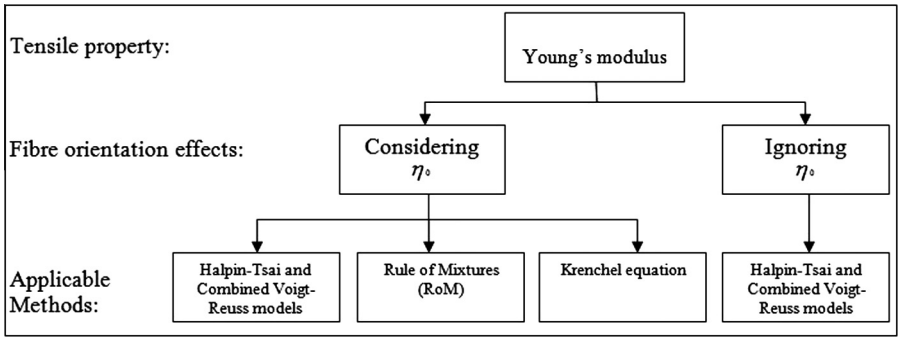

Fig. 6. Schematic diagram showing a flow chart of the methodology used to evaluate the Young's modulus of CNT-CF/PP composite.

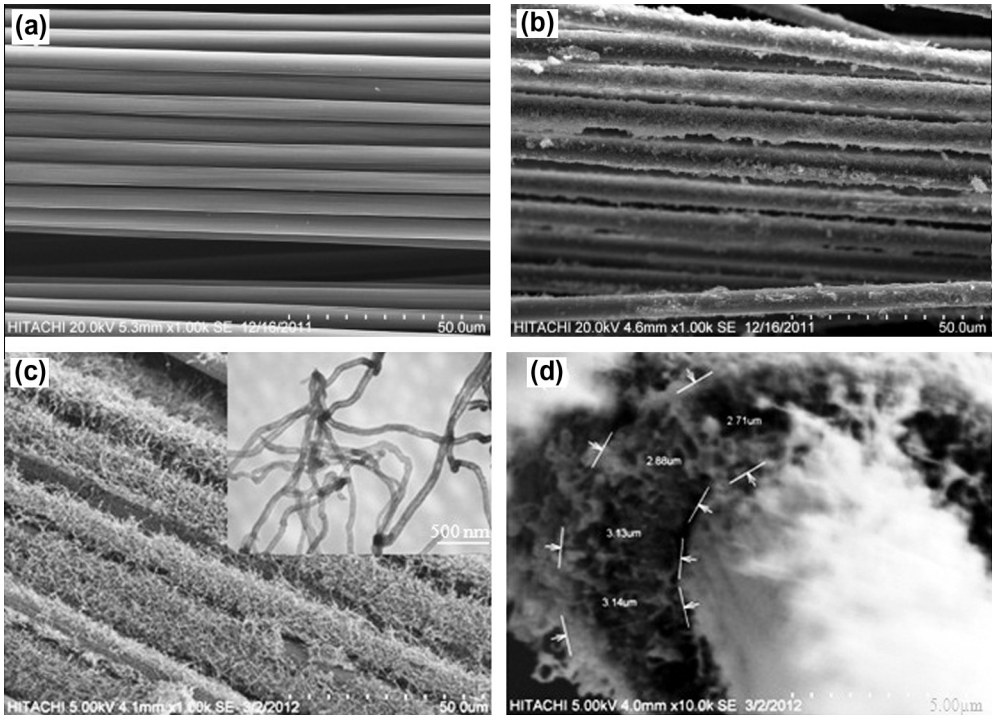

Fig. 7. Representative SEM images (a) as received CF, (b) CNT coated CF at 800 °C, (c) CNT coated CF at 700 °C (inset shows representative TEM image of CNT on the coating surface), and (d) measurement of CNT coating thickness over CF.

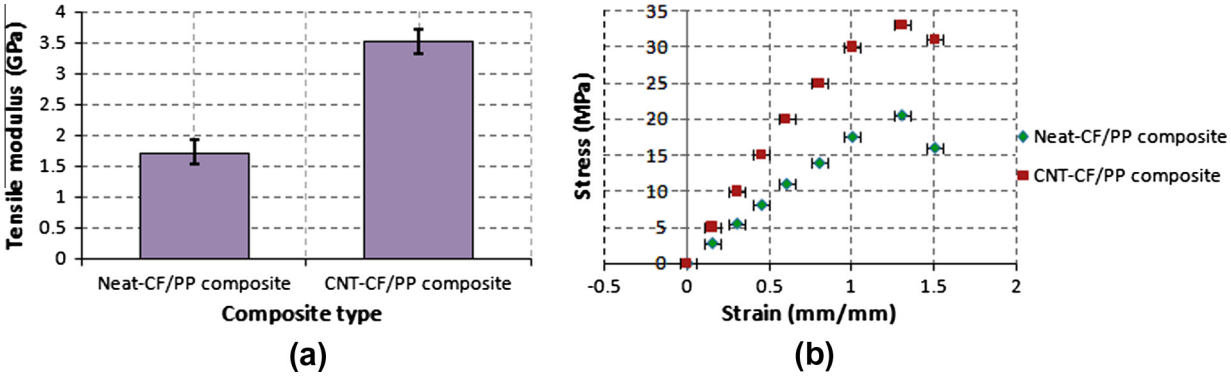

Fig. 8. Tensile behavior of neat-CF/PP and CNT-CF/PP composites, (a) tensile modulus and (b) stress vs. strain curves representing tensile strength (error bars denote the standard deviation of the measurement).

direction to the tensile loading which is normal to the fracture surface.

A fibre orientation distribution function was represented with the inclination angles which have the property such that the variation of its function's shape parameters is able to describe a change from a unidirectional distribution to a random distribution. Table 2 shows the fibre orientation angles with corresponding numerical values which are essential for calculating the fibre orientation cefficiency factor η_0.

3.4. Model based prediction of nanocomposite tensile properties

According to the dynamic system modeling when fixed 'Halpin and Tsai' and 'Combined Voigt–Reuss' describes the time dependence of system environment, the strain value was changed under application of increasing stress. Young's modulus of CNT reinforced PP (CNT/PP) composite was predicted through Eq. (6). By using Eqs. (1) and (2), the longitudinal and transverse modulus of CNT-CF/PP composites was evaluated which was further utilized to calculate the overall tensile modulus through Eq. (3).

The calculations are conducted by using the data quoted in Table 1 and the step by step procedure follows:

From Eq. (6),	Young's modulus of CNT/PP composite, E_M = 1.55 GPa

The value of E_M was then utilized as the model CNT/PP matrix where CF was considered as the reinforcement inside the hybrid composite.

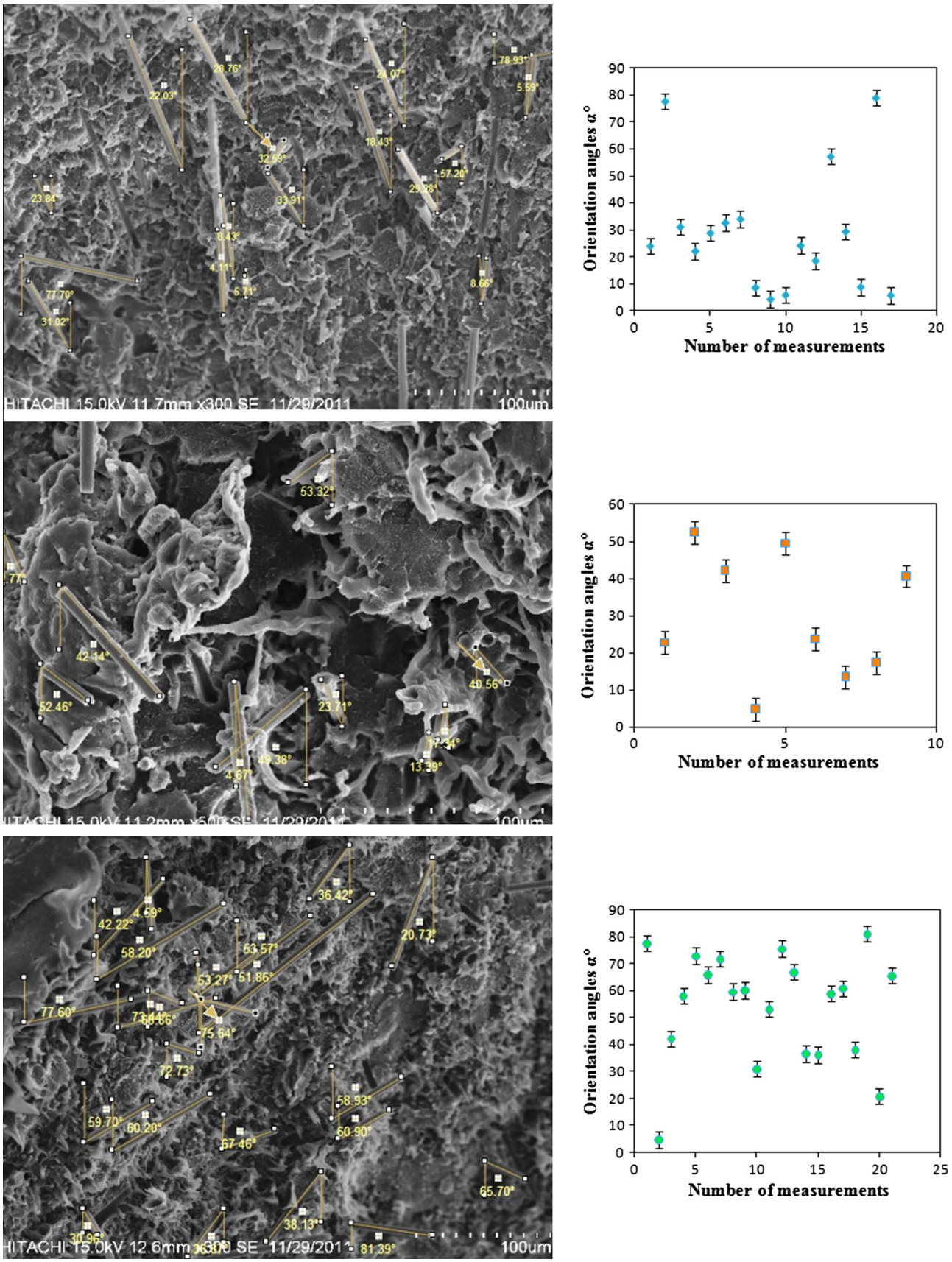

Fig. 9. Fibre orientation geometry on the fractured surfaces of different CNT-CF/PP composites subjected to tensile test with the orientation angles distribution.

Table 2
Fibre orientation efficiency determined from different composite samples.

Field of view	Average α (°)	Number of fibres	N_f	$N_f \cos^3\alpha$	$N_f \sec\alpha$	$N_f \cos^4\alpha$
1	28.83	17	0.12	0.080	0.136	0.070
2	31.97	10	0.07	0.044	0.082	0.036
3	54.40	23	0.16	0.031	0.275	0.018
4	45.78	25	0.18	0.060	0.258	0.042
5	39.47	13	0.09	0.042	0.116	0.032
6	53.58	18	0.13	0.027	0.220	0.016
7	42.73	16	0.11	0.043	0.150	0.032
8	39.73	17	0.12	0.054	0.156	0.042
	Average = 42.05	$\sum$ = 139	$\sum$ = 1	$\sum$ = 0.381	$\sum$ = 1.390	$\sum$ = 0.288

From Eq. (1),	Longitudinal efficiency factor, η_{11} = 0.181 Longitudinal modulus of CNT-coated CF reinforced PP composite, E_{11} = 11.40 GPa
From Eq. (2),	Transverse efficiency factors, $\eta_{\perp}$ = 0.992 Transverse modulus of CNT-coated CF reinforced PP composite, $E_{\perp}$ = 1.65 GPa
From Eq. (3),	Young's modulus for CNT-CF/PP composites, E_C = 5.31 GPa

Tensile strength is the maximum stress that the composite can withstand before failing or breaking. From the stress–strain relation where Young's modulus acts as the initial gradient of the straight portion of the curve, tensile strength was found 53.10 MPa.

When η_0 is a concern, Young's modulus was found to be 4.57 GPa and the corresponding tensile strength was 45.70 MPa. Fig. 10 shows the deviation between the experimental findings and theoretical evaluation. The experimental findings of the tensile properties of neat-CF/PP composite were considered as the baseline when comparing between the results found from different scheme. In contrast with the neat-CF/PP a composite, the tensile modulus of CNT-CF/PP composites was enhanced by approximately 104% and tensile strength increased to approximately 64%. The enhanced tensile properties are likely to be the overall effect of CF surface coating by CNT. CNT have dominated as the interfacial binder in between the CF and PP matrix; as well as being the additional supporting reinforcement for the hybrid composites. In the context of this approach, when the fibre orientation effect is ignored anoteworthy increase in tensile modulus with 51% was obtained rather than experimental result of CNT-CF/PP composite. When η_0 is considered a more acceptable validation with the experimental results was obtained which shows a moderate increase with 30% in the predicted value. The results can be compared to the outcomes as demonstrated by Kulkarniand coworkers where the numerical analysis predicted the elastic modulusin the transverse direction to be about 1.4 times the experimentally determined value [34].

Under different applied stress CNT-CF/PP composites have shown different strain values while algorithms are implemented through numerical computing environment. Strain values are the results of calculations in interactive mode as Young's modulus of elasticity is the ratio between stress and strain. In the case of anisotropic materials, Young's modulus will change depending on the direction from which the force is applied. Table 3 shows the variations in a sequential way.

Comparative behaviors of CF/PP and CNT-CF/PP composite tensile properties are shown in Fig. 11. The plot shows a significant variation in between the experimental and theoretical results in terms of resulted strain values under application of increasing stress.

The variations between the experimental and estimated values are considered due to the experimental errors. When ignoring the fibre orientation distribution, it has been assumed that in a unit volume of composite all the differently oriented fibres have equal average fibre length, and the fibres are transversely oriented within a unit volume of the composite. A better correlation has been found when fibre orientation efficiency in considered. Since the fibre orientation distribution was measured only at the transverse

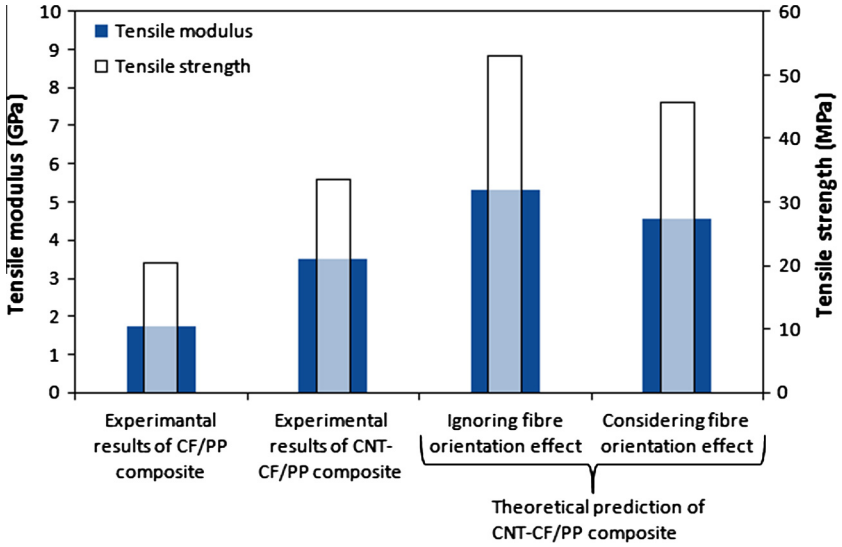

Fig. 10. Deviation in tensile behavior of CF/PP to CNT-CF/PP composites under experimental observation and theoretical prediction.

Table 3
Elastic response of neat-CF/PP and CNT-CF/PP composite based on experimental and theoretical predictions.

Neat CF/PP composite		CNT-CF/PP composite			
Applied stress (MPa)	Observed strain (mm/mm) (experimental)	Applied stress (MPa)	Observed strain (mm/mm) (experimental)	Predicted strain (mm/mm) (ignoring η_0)	Predicted strain (mm/mm) (considering η_0)
2.8	0.15	5	0.15	0.10	0.11
5.5	0.30	10	0.30	0.20	0.22
8.1	0.45	15	0.45	0.30	0.33
11	0.60	20	0.60	0.40	0.44
13.9	0.80	25	0.80	0.53	0.58
17.5	1.00	30	1.00	0.66	0.72
20.5	1.30	33	1.30	0.85	0.94
16	1.50	31	1.50	0.97	1.08

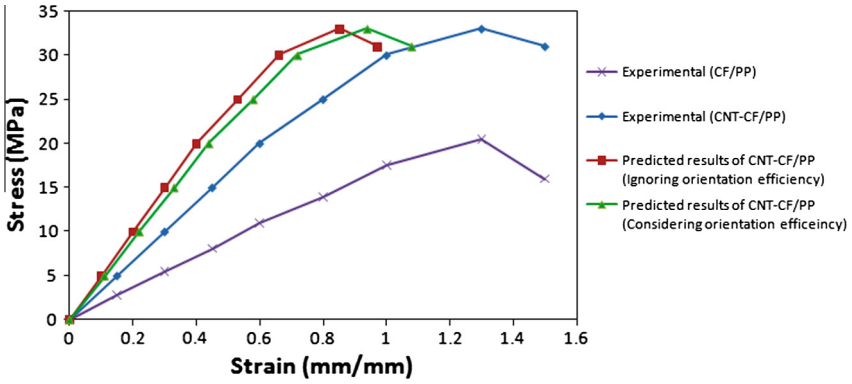

Fig. 11. Comparative stress vs. strain curves representing elastic behavior of CF/PP composite in contrast to CNT-CF/PP composite obtained through experimental observations and theoretical prediction.

direction to the tensile loading, the value of η_0 was implemented to determine the transverse modulus on the course of overall modulus determination.

4. Conclusions

It was demonstrated that the CVD method was able to grow CNT on the surface of CF when appropriate CNT growth condition are used. The evidence of intensive CNT-coating on CF was shown by using SEM at a CVD temperature of 700 °C and 30 min reaction time. With a similar reaction condition, CNT-coated CF was shown to be significant with elevated tensile properties of CNT-CF/PP hybrid composite. The procedure was conducted by using the tensile test on the fabricated samples of randomly oriented short fibre reinforced composites. In contrast with the neat-CF/PP composite, CNT-CF/PP composite has shown enhanced Young's modulus by approximately 104% and tensile strength increased to approximately 64%. The justification of supreme tensile properties of hybrid composite was explained to be dependent on fibre–matrix adhesion incorporated by interfacial CNT.

A hierarchical model comprising Halpin–Tsai equations, combined Voigt–Reuss model, simple rule-of-mixtures (RoMs) and Krenchel approach was then utilized to evaluate the overall tensile properties of CNT-CF/PP composite. Initially, CF orientation distribution geometry inside the composite was overlooked relying on the calculated transverse and longitudinal modulus. Young's modulus for CNT-CF/PP composite regardless of fibre orientation was found to be approximately 5.31 GPa and the tensile strength was estimated to be 53.10 MPa. Afterward, the randomness of short CF was investigated through fractographic study of the composite fracture surface by using SEM. A comprehensive analysis was conducted on the fibres of fracture surface by using Bersoft and Geozebra image analyzing software packages to evaluate the fibre orientation distribution factor, η_0. With this perspective, Young's modulus was obtained to be approximately 4.57 GPa and the corresponding tensile strength was 45.70 MPa. Regardless of fibre randomness, a noteworthy deviation in tensile modulus of CNT-CF/PP composite with 51% was notified compared to the experimental result. When η_0 is considered a more satisfactory validation with the experimental results was obtained which shows a modest deviation with 30% to the predicted Young's modulus.

Acknowledgments

The authors would like to acknowledge the financial support given by Universiti Putra Malaysia underthe Research University Grant Scheme and Ministry of Science, Technology and Innovation, Malaysia (MOSTI) under the Brain Gain R&D program.

References

[1] Kalaprasad G, Thornas S. Hybrid fibre reinforced polymer composites. Int Plast Eng Technol 1995;1:87–98.
[2] Fu S-Y, Lauke B, Mai Y-W. Science and engineering of short fibre reinforced polymer composites. Woodhead: Plastic Information Direct; 2009.
[3] Tang LG, Kardos JL. A review of methods for improving the interfacial adhesion between carbon fiber and polymer matrix. Polym Compos 1997;18:100–13.
[4] Godara A, Gorbatikh L, Kalinka G, Warrier A, Rochez O, Mezzo L, et al. Interfacial shear strength of a glass fiber/epoxy bonding in composites modified with carbon nanotubes. Compos Sci Technol 2010;70:1346–52.
[5] Yamamoto N, John Hart A, Garcia EJ, Wicks SS, Duong HM, Slocum AH, et al. High-yield growth and morphology control of aligned carbon nanotubes on ceramic fibers for multifunctional enhancement of structural composites. Carbon 2009;47:551–60.

[6] Rezaei F, Yunus R, Ibrahim NA. Effect of fiber length on thermomechanical properties of short carbon fiber reinforced polypropylene composites. Mater Des 2009;30(2):260–3.
[7] Carneiro OS, Maia JM. Rheological behavior of (short) carbon fiber/thermoplastic composites. Part I: the influence of fiber type, processing conditions and level of incorporation. Polym Compos 2000;21(6):960–9.
[8] Fu SY, Lauke B, Mäder E, Yue CY, Hu X. Tensile properties of short-glass-fiber- and short-carbon-fiber-reinforced polypropylene composites. Composites Part A: Appl Sci Manufac 2000;31(10):1117–25.
[9] Colin MS. Elastic anisotropy of short-fibre reinforced composites. Int J Solids Struct 1992;29(23):2933–44.
[10] Suraya AR, Christina V, Robiah Y, Shamsudin S. CVD whiskerization treatment process for the enhancement of carbon fiber composite flexural strength. Pertanika J Sci Technol 2008;16(1):73–81.
[11] Qiuhong Z, Jianwei L, Ryan S, Liming D, Jeffery B. Hierarchical composites of carbon nanotubes on carbon fiber: influence of growth condition on fiber tensile properties. Compos Sci Technol 2009;69:594–601.
[12] Botelho EC, Figiel L, Rezende MC, Lauke B. Mechanical behavior of carbon fiber reinforced polyamidecomposites. Compos Sci Technol 2003;63(13):1843–55.
[13] Dumont P, Orgéas L, Favier D, Pizette P, Venet C. Compression moulding of SMC: in situ experiments, modelling and simulation. Composites: Part A 2007;38(2):353–68.
[14] Rahmanian S, Thean KS, Suraya AR, Shazed MA, Mohd Salleh MA, Yusoff HM. Carbon and glass hierarchical fibers: influence of carbon nanotubes on tensile, flexural and impact properties of short fiber reinforced composites. Mater Des 2013;43:10–6.
[15] Martin C. Tensile testing: a simple introduction. Phys Educ 2006;41(1):001–5.
[16] Bakshi SR, Lahiri D, Agarwal A. Carbon nanotube reinforced metal matrix composites – a review. Int Mater Rev 2010;55:41–63.
[17] Halpin JC, Pagano NJ. The laminate approximation for randomly oriented fibrous omposites. J Compos Mater 1969;3(2):720.
[18] Halpin JC, Kardos JL. The Halpin–Tsai equations: a review. Polym Eng Sci 1976;16:344–52.
[19] Halpin JC, Tsai SW. In: Air force material laboratory technical, report; 1967 [AFML-TR-67-423].
[20] Roderic L. Composite biomaterials: chapter one, The Biomedical Engineering Handbook. 2nd ed. University of Wisconsin-Madison; 2000. p. 40.1–7.
[21] Tsai SW, Adams DF, Doner DR. Analyses of composite structures. Technical Report for NASA; 1966 [CR-620].
[22] Mishnaevsky Jr L. A simple method and program for the analysis of the microstructure-stiffness interrelations of composite materials. J Compos Mater 2007;41:73–87.
[23] Abderrahmane M, Jalel A, Abdellatif A, Robert G. Micromechanical modeling of tensile behavior of short fiber composites. J Compos Mater 2002;36:423–41.
[24] Sulaiman S, Yunus R, Ibrahim NA, Rezaei F. Evaluation of carbon vapour deposition technique from whiskerization treatment of carbon fibers. Int J Eng Technol 2006;3:85–90.
[25] Hui Q, Alexander B, Emile SG, Milo SP. Carbon nanotube grafted carbon fibres: a study of wetting and fibre fragmentation. Compos: Part A 2010;41:1107–14.
[26] Myungsoo K, Young-Bin P, Okenwa IO, Chuck Z. Processing, characterization, and modeling of carbon nanotube-reinforced multiscale composites. Compos Sci Technol 2009;69:335–42.
[27] Lubineau G, Rahaman A. A review of strategies for improving the degradation properties of laminated continuous-fiber/epoxy composites with carbon-based nanoreinforcements. Carbon 2012;50:2377–95.
[28] Mohammad AR, Javad R, Zhou W, Huaihe S, Zhong-Zhen Y, Nikhil K. Enhanced mechanical properties of nanocomposites at low graphene content. ACS Nano 2009;3(12):3884–90.
[29] Mathur RB, Chatterjee S, Singh BP. Growth of carbon nanotubes on carbon fibre substrates to produce hybrid/phenolic composites with improved mechanical properties. Compos Sci Technol 2008;68:1608–15.
[30] Mukul K, Yoshinori A. Chemical vapor deposition of carbon nanotubes: a review on growthmechanism and mass production. J Nanosci Nanotechnol 2010;10:3739–58.
[31] Qiang Z, Weizhong Q, Rong X, Zhou Y, Guohua L, Yao W, et al. In situ growth of carbon nanotubes on inorganic fibers with different surface properties. Mater Chem Phys 2008;107(2–3):317–21.
[32] Sharma SP, Lakkad SC. Effect of CNT growth on carbon fibers on the tensile strength of CNT growncarbon fiber-reinforced polymer matrix composites. Compos: Part A 2011;42:8–15.
[33] Laspalas M, Crespo C, Jiménez MA, García B, Pelegay JL. Application of micromechanical models for elasticity and failure to short fibre reinforced composites. Numerical implementation and experimental validation. Comput Struct 2008;86:977–87.
[34] Kulkarni M, Carnahan D, Kulkarni K, Qian, Abot JL. Elastic response of a carbon nanotube fiber reinforced polymeric composite:A numerical and experimental study. Compos: Part B 2010;41:414–21.